# Topological Analysis of Fluorinated Dimethyl Ethers and Their Protonated Forms

**Antonio Vila[†] and Ricardo A. Mosquera*[,‡]**

*Departamento de Física Aplicada, Universidade de Vigo, Facultade de Ciencias do Campus de Ourense, E 32004 Ourense, Spain, and Departamento de Química Física, Universidade de Vigo, Facultade de Ciencias do Campus de Vigo, E 36200 Vigo, Spain*

*Received: July 31, 2000*

Changes induced by stepwise substitution of hydrogen for fluorine in neutral and protonated dimethyl ethers are analyzed in the light of the Atoms in Molecules (AIM) theory. AIM atomic and bond properties were computed by using B3LYP/6-31++G(d,p)//B3LYP/6-31G(d,p) wave functions. The effects brought about by fluorine substitution on the atomic and bond properties of the C−O−C chain were analyzed. Fluorine substitution was found to strengthen the C−H bonds. The computed proton affinities were related to the charge and energy of the proton. Reorientation of the $CF_nH_{3-n}$ groups upon protonation was explained in terms of the balance between anomeric and steric interactions. This interpretation and lacking of F−H bond paths allow the rejection of the previously proposed hydrogen bonding O−H···F linkages in these systems. The fluorine substitution destabilizes C atoms in neutral and protonated forms, whereas the O is stabilized in the neutral molecule and destabilized in the cation.

## 1. Introduction

After signing of the Montreal Protocol[1] on September 1987, which sets the elimination of ozone depletion substances as its final objective, research into chlorofluorocarbons (CFCs) alternatives became very active. CFCs were considered as important contributors to the depletion of the ozone layer, because of their long atmospheric lifetime. Hydrofluorocarbons (HFCs) were proposed as an alternative to CFCs. Because of the lack of chlorine, HFCs do not contribute directly to the ozone depletion, but their reactivity with free hydroxyl radicals is not as good as desired. The strategy of introducing oxygen into an HFC usually, though not always, leads to an enhancement of its reactivity with hydroxyl radicals, by weakening the adjacent C−H bonds, thereby reducing their contribution to global warming.[2]

A number of theoretical and experimental studies have been performed in order to determine the potential reactivity of hydrofluoroethers. In a theoretical kinetic study employing DFT calculations, Bartolotti et al.[3] concluded that hydroxyl reactivity of hydrofluoroethers (HFEs) decreases as fluorine atoms replace hydrogens. A theoretical study of the C−H bond strength of fluorinated dimethyl ethers has also shown that heavily F-substituted dimethyl ethers possess stronger C−H bonds that that their fluorethane counterparts.[4] In another paper, Good et al.[5] have also measured the lifetimes and warming potentials of fluorinated ethers, showing that increasing fluorination is accompanied by slower rates of reaction with hydroxyl radicals and ultimately longer lifetimes.

Ab initio molecular structures have been reported on neutral $CH_3OCF_3$,[6] $(CH_2F)_2O$,[7] $(CHF_2)_2O$,[6,7] $(CF_3)_2O$,[7−9] and $(CH_3)_2O$[7,8] and protonated $(CH_2F)_2OH^+$,[7] $(CHF_2)_2OH^+$,[7] $(CF_3)_2OH^+$,[7,8] and $(CH_3)_2OH$.[7,8] The aim of the present paper is 3-fold: (i) to perform a study of the structure and proton affinities of the whole series of fluorinated dimethyl ethers, since the available work deals only with part of this series; (ii) to systematically examine the effects of stepwise fluorination on the atomic and bond properties of fluorinated dimethyl ethers; (iii) as the systems under consideration present a different number of C−O−C−F anomeric units, this work also deals with the interpretation of the anomeric effect in the light of the AIM theory.

The anomeric effect can be defined as the gauche conformational preference exhibited by R−X-A−Y units, where X is an atom with lone pairs (lp), A is an atom with intermediate electronegativity, and Y is more electronegative than A (as it is the case in C−O−C−F).[10] Though the first description of the anomeric effect was presented 45 years ago,[11] its explanation has been a source of controversy in chemical literature.[12] Several models have been employed to study the origin of the conformational preference;[11−13] however, electrostatic interactions and charge delocalization models seem to be the most widely employed. Studies on several systems by using natural bond orbital analysis (NBO) to analyze the delocalization effect[12,14−15] pointed to a complex origin of the generalized anomeric effect, that cannot be rationalized in terms of the electrostatic theory, where delocalizations (of which $n_X \rightarrow \sigma^*_{C-Y}$ hyperconjugation is only one contribution) play a crucial role. The Theory of Atoms in Molecules[16] (AIM) was also applied to study the anomeric effect in dimethoxymethane.[17] The results of this study, which included a topological analysis of the Laplacian of the charge density, were not in keeping with the view that O−C−O anomeric effect derives exclusively from $n_X \rightarrow \sigma^*_{C-Y}$ charge delocalization.

## 2. Theory of Atoms in Molecules

The theory of atoms in molecules is an extension of quantum mechanics to subdomains which allows one to split a molecule into its constituent atoms full-filling quantum-mechanical postulates.[16,18] This division is achieved by the zero flux boundary condition of the vector field of the gradient of the charge density. This condition can be derived in strict terms

[†] Departamento de Física Aplicada.
[‡] Departamento de Química Física.

10.1021/jp002725v CCC: $19.00 
Published on Web 12/05/2000

**TABLE 1: Total Energies, Virial Coefficients, and Errors in the Integration: See Text for Details**

| | compound[a] | $E$ (au) | $\gamma = -V/T$ | $E - \sum E(\Omega)$ (kJ mol$^{-1}$) | $N - \sum N(\Omega)$ (au) | $\sum L(\Omega)$ (au) |
|---|---|---|---|---|---|---|
| **1** | $CH_3OCH_3$ | −155.04135 | 2.00955 | 1.21 | 0.0019 | 0.0014 |
| **2** | $CH_3OCH_2F$ | −254.29221 | 2.00859 | 2.42 | 0.0037 | 0.0038 |
| **2t** | $CH_3OCH_2F$ (anti) | −254.28412 | 2.00859 | −0.28 | 0.0009 | 0.0007 |
| **3** | $CH_3OCHF_2$ | −353.54733 | 2.00815 | −0.41 | 0.0012 | 0.0012 |
| **4** | $CH_3OCF_3$ | −452.79798 | 2.00793 | 0.81 | 0.0042 | 0.0058 |
| **5** | $CH_2FOCH_2F$ | −353.53782 | 2.00817 | 1.13 | 0.0025 | 0.0031 |
| **6** | $CH_2FOCHF_2$ | −452.78896 | 2.00792 | 0.05 | 0.0000 | −0.0004 |
| **7** | $CH_2FOCF_3$ | −552.03834 | 2.00778 | −2.20 | −0.0042 | −0.0064 |
| **8** | $CHF_2OCHF_2$ | −552.03521 | 2.00777 | 1.45 | 0.0038 | 0.0053 |
| **9** | $CHF_2OCF_3$ | −651.28449 | 2.00767 | 1.60 | 0.0031 | 0.0043 |
| **10** | $CF_3OCF_3$ | −750.53195 | 2.00761 | 1.66 | 0.0037 | 0.0055 |
| **1**+ | $CH_3OH^+CH_3$ | −155.35427 | 2.00964 | 0.34 | 0.0002 | 0.0001 |
| **2**+**(a)** | $CH_3OH^+CH_2F$ | −254.58526 | 2.00865 | −0.21 | −0.0008 | −0.0012 |
| **2**+**(b)** | | −254.58146 | 2.00865 | 0.04 | −0.0007 | −0.0009 |
| **3**+ | $CH_3OH^+CHF_2$ | −353.82377 | 2.00820 | −0.60 | −0.0004 | −0.0008 |
| **4**+ | $CH_3OH^+CF_3$ | −453.06154 | 2.00797 | 2.71 | 0.0033 | 0.0046 |
| **5**+ | $CH_2FOH^+CH_2F$ | −353.81249 | 2.00822 | 1.50 | 0.0020 | 0.0026 |
| **6**+**(a)** | $CH_2FOH^+CHF_2$ | −453.05193 | 2.00797 | 0.51 | 0.0002 | 0.0004 |
| **6**+**(b)** | | −453.04926 | 2.00797 | 2.55 | 0.0020 | 0.0030 |
| **7**+**(a)** | $CH_2FOH^+CF_3$ | −552.28922 | 2.00783 | −0.26 | −0.0021 | −0.0032 |
| **7**+**(b)** | | −552.28592 | 2.00783 | 1.13 | −0.0004 | −0.0001 |
| **8**+ | $CHF_2OH^+CHF_2$ | −552.29000 | 2.00782 | 3.35 | 0.0062 | 0.0090 |
| **9**+ | $CHF_2OH^+CF_3$ | −651.52535 | 2.00772 | −2.05 | −0.0029 | −0.0051 |
| **10**+ | $CF_3OH^+CF_3$ | −750.76170 | 2.00765 | 3.13 | 0.0074 | 0.0105 |

[a] In the protonated species (a) and (b) denote two non equivalent forms: In (a) proton is at the same side of the COC plane that the fluorine atom bonded to the monohalogenated C. When both carbons are monohalogenated (a) denotes the protonated form in which proton and fluorine bonded to C1 are at the same side of the COC plane.

from Schwinger's principle of stationary action.[19] Each of the fragments thus obtained possesses an attractor (usually a nucleus) for the charge density and a basin, $\Omega$, throughout which trajectories of $\nabla\rho$ spread. For every property, $P$, represented by the operator $\hat{P}$, its atomic value, $P(\Omega)$, is obtained by integrating the corresponding three-dimensional property density $\rho_P$ (eq 1) over the basin of the atom (eq 2). The atomic basins are well-defined quantum subspaces, wherein the virial theorem holds, and atomic contributions can be added up to obtain the value of the overall system (eq 3).[20] Properties of interest for the work reported here are the electron population of an atom, $N(\Omega)$, and total energy, $E(\Omega)$. $N(\Omega)$ is obtained by integrating the electron charge density over the atomic basin. For molecules in equilibrium geometries $E(\Omega)$ is provided by the integration of the kinetic energy density function. For convenience, we have also used the net charge of an atom, $q(\Omega)$, which is defined as its nuclear charge minus its basin electron population.

$$\rho(\vec{r}) = \frac{N}{2}\int d\tau'\{\psi^*(\vec{r})\hat{P}\psi(\vec{r}) + [\hat{P}\psi(\vec{r})]^*\psi(\vec{r})\} \quad (1)$$

$$P(\Omega) = \int_\Omega d\tau\ \rho_P(\vec{r}) \quad (2)$$

$$P = \sum_\Omega P(\Omega) \quad (3)$$

Along the bond path connecting two bonded atoms there exists a (3,−1) critical point for the charge density, known as a bond critical point. Various properties at this point are also of interest: charge density, $\rho_c$; eigenvalues of the Hessian of the charge density, $\lambda_1 < \lambda_2 < \lambda_3$; ellipticity of the bond, $\epsilon = \lambda_1/\lambda_2 - 1$ and the total energy density, $H_c$.

### 3. Computational Details

All the molecular orbital calculations on the molecules here studied (Table 1) were performed with the GAUSSIAN 94[21] programs package using Kohn−Sham orbital density functional theory (DFT).[22] Becke's three parameter functional[23] with the nonlocal correlation provided by Lee, Yang, and Parr[24] (B3LYP) was used in all instances. Geometry optimizations were undertaken with the 6-31G(d,p) Gaussian type basis. The resulting geometries were then used in a single point energy calculation to obtain the corresponding wave functions and energies at the B3LYP/6-31++G(d,p) level.

For the partially fluorinated ethers, F atoms were placed in the way they presented the largest number of gauche dispositions with regard to the C−O−C plane. It has been checked that this is the lowest energy conformation. For example, the molecule $CH_3OCH_2F$ with fluorine atom in trans arrangement (denoted in Tables as **2t**) was calculated to be less stable by 21 kJ mol$^{-1}$ than its gauche conformer at this computational level. This agrees with the far-infrared spectrum of gaseous fluoromethyl methyl ether, **2,** obtained by Durig et al.[25] which showed no evidence for the high energy trans conformer. It is also in agreement with the conformational preference that could be predicted according to the anomeric effect. In molecule **5**, fluorine atoms were placed at opposite sides of the C−O−C plane. This was also checked to be the most stable rotamer.

The proton affinities (PAs)[26,27] were estimated by taking the energy difference between the protonated and neutral forms. In this work, none of the energy calculations were explicitly corrected for zero-point vibrational energy (ZPVE), as the near constancy of the difference of ZPVE between the protonated and neutral forms was previously found[28] and only relative values are needed for our purposes. The topological analysis of charge distribution and numerical integrations over atomic basins were carried out by using the AIMPAC[29] program series. For those systems where asymmetric fluorination gives rise to two different protonations, we have computed the energy for both protonated forms (denoted as **a** and **b** in Table 1). We have always found that the protonated form with more anti lp-O−C−F antiperiplanar arrangements was the most stable, as could be expected according to anomeric interactions.

**TABLE 2: Bond Lengths (angstroms) and Angles (degrees) in Neutral (M) and Most Stable Protonated ($MH^+$) Species**

| | M | | | $MH^+$ | | | |
|---|---|---|---|---|---|---|---|
| complex | $r_{O-C1}$ | $r_{O-C2}$ | $\alpha_{C1-O-C2}$ | $r_{O-C1}$ | $r_{O-C2}$ | $\alpha_{C1-O-C2}$ | $w_{F-C1-C2-F}$[a] |
| **1** | 1.410 | 1.410 | 112.3 | 1.495 | 1.495 | 117.5 | |
| **2** | 1.425 | 1.376 | 113.7 | 1.509 | 1.501 | 117.1 | |
| **2t** | 1.415 | 1.392 | 112.6 | | | | |
| **3** | 1.438 | 1.354 | 115.3 | 1.517 | 1.521 | 117.8 | |
| **4** | 1.438 | 1.345 | 115.4 | 1.517 | 1.511 | 118.8 | |
| **5** | 1.395 | 1.395 | 114.2 | 1.511 | 1.539 | 116.5 | 1 |
| **6** | 1.409 | 1.370 | 116.1 | 1.528 | 1.551 | 119.4 | 16 |
| **7** | 1.412 | 1.361 | 116.5 | 1.539 | 1.529 | 119.7 | 2 |
| **8** | 1.387 | 1.387 | 120.8 | 1.565 | 1.539 | 119.8 | 89, 97 |
| **9** | 1.391 | 1.376 | 120.4 | 1.582 | 1.539 | 121.3 | 34, 36 |
| **10** | 1.381 | 1.381 | 120.2 | 1.556 | 1.559 | 121.9 | 21, 32 |

[a] $w_{F-C1--C2-F}$ are the absolute values displayed by the dihedral angles formed by the F−C bonds which are eclipsed in the unprotonated species. Two values are indicated for those molecules with two C−F bonds eclipsed in the most stable rotamer of the neutral form.

## 4. Results and Discussion

Energies of neutral and protonated forms are shown in Table 1. It also displays virial ratios and integrations errors expressed as differences between total properties and those obtained by summation of the properties of fragments [$N - \Sigma N(\Omega)$, $E - \Sigma E(\Omega)$] and the summation of the integrated values of the Laplacian of the charge density over all the atomic fragments [$\Sigma L(\Omega)$]. This value indicates the precision with which the surfaces of zero flux have been determined, and hence, the precision for the integrated properties calculated for the fragment. Atomic charges add up to an average of 0.003 au with a maximum value of 0.007 au and the average energy discrepancy with the total energy has been of 1.4 kJ $mol^{-1}$ with a maximum value of 3.2 kJ $mol^{-1}$. These errors are acceptable for our purposes.

The electron populations, $N(\Omega)$, are influenced by the accuracy within the zero flux surface has been determined, expressed by the integrated value of the Laplacian of the charge density in the fragment, $L(\Omega)$. An excellent degree of correlation ($r^2 = 0.989$) is found between the summation of the $L(\Omega)$ values and the error in the additivity of the electron populations $N$-$\Sigma N(\Omega)$, as was shown in previous works.[30,31]

**A. Geometries.** Optimized C−O bond lengths and C−O−C bond angles for the neutral and protonated species are gathered in Table 2. To the authors' knowledge, experimental structures are only available for $(CH_3)_2O$ and $CH_2FOCH_3$ molecules. The electron diffraction data for $(CH_3)_2O$[32] ($r_{CO} = 1.410$ Å and $\alpha_{COC} = 111.7°$) compare well with the calculated geometrical parameters optimized at the B3LYP/6-31G(d,p) level. For the molecule $CH_2FOCH_3$, microwave spectroscopy yielded the values $r_{C2O} = 1.368$ Å, $r_{C1O} = 1.426$ Å, and $\alpha_{C1OC2} = 113.5°$,[25] which also show a reasonable good agreement with the optimized values, bearing in mind the different physical meaning of the $r^0$ and $r_e$ structures.[33]

Because of the strong electron-withdrawing nature of fluorine atoms, F substitution leads to a substantial shortening of the C−O bonds, as it can be seen from Table 2. To analyze the effect of the progressive fluorination on C−O bond distances, Figure 1 shows a plot of the $r_{C1O} + r_{C2O}$ combined bond distances against the number of fluorine atoms in the complex. The combined bond distances are found to decrease in a nonlinear manner as the number of fluorine atoms increases. This is a consequence of the reduction of the oxygen atomic basin imposed by the non additive inductive effect of the nearby fluorine atoms.[34,35] Molecules with equal number of fluorine

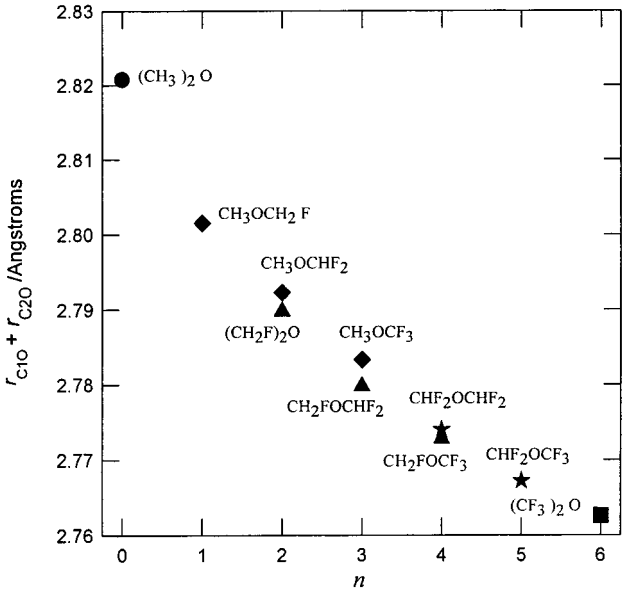


**Figure 1.** Combined CO bond distances ($r_{C1O}+r_{C2O}$) in fluorinated dimethyl ethers versus the number of fluorine atoms $n$ in the molecule. (●) $(CH_3)_2O$, (◆) $CH_3OCH_{3-n}F_n$, (▲) $CH_2FOCH_{3-m}F_m$, (★) $CHF_2OCH_{3-l}F_l$, (■) $(CF_3)_2O$.

atoms have different combined bond distances, according to the different dihedral angles of fluorine atoms with regard to the C−O−C molecular plane. This is also true for different conformers of the same molecule (trans and gauche conformers of compound **2**). It is a well-known fact that F−C bonds trans to an oxygen lone pair are lengthened by anomeric interactions.[10,13] In fact, O−$C_2$ bond is shortened by 0.016 Å in the gauche conformer of **2** with regards to the trans conformer (Table 2), whereas the C−F bond length lengthens from 1.365 Å in the trans conformer to 1.391 Å in the gauche. The simultaneous, significant, and opposite variations of O−$C_2$ and $C_2$−F between **2** and **2t** bond lengths can be ascribed to a $n_O \rightarrow \sigma^*_{C-F}$ hyperconjugative delocalization.

The addition of more electron-withdrawing fluorine atoms results in differing C−O bond lengths. Holding the fluorine content on $C_1$ fixed at any value and increasing the fluorine content of $C_2$, $C_1$−O bonds are appreciably stretched while $C_2$−O bonds are shortened. $C_1$−O stretching is a consequence of more electron density being pulled up to the $C_2$ group because of its increased fluorine content.

On going from $C_1X$−O−$C_2H_2F$ to $C_1X$−O−$C_2HF_2$, $C_2$−O bond length exhibits a drop of about 0.02 Å, while fully fluorination on $C_2$ leads to a drop of about 0.01 Å on $C_2$−O bond distance. As noted above, the latest F-substitution on $C_2$ corresponds to the hydrogen atom in trans position, where the shortening of the $C_2$−O bond length is not favored by anomeric interactions.

The calculated C−O−C bond angle is also found to increase as hydrogens in gauche arrangement to the C−O−C unit are replaced by fluorine atoms. The variations presented by this bond angle when anti hydrogens are replaced by fluorine are much smaller. The evolution of the C−O−C bond angle can be interpreted as the combined result of anomeric and steric effects. In fact, the optimized values of this angle (Table 2) increase as the number of anomeric C−O−C−F arrangements that favor a $n_O \rightarrow \sigma^*_{C-F}$ hyperconjugative delocalization (gauche arrangement) increases: zero in molecules **1** and **2t**, one in molecule **1**, two in molecules **3**-**5**, three in molecules **6**-**7**, and four in molecules **8**-**10**. The magnitude of the steric interactions depleted when the angle C−O−C is opened is expected to

**TABLE 3: Calculated Properties at the C−H Bond Critical Point. Distances in angstroms and the Remaining Properties in au**

| compound | $r_{CH}$ | $\rho_c$ | $H_c$ |
|---|---|---|---|
| $CH_3OCH_2-H$ | 1.093 | 0.2855 | −0.2973 |
| $CH_2FOCH_2-H$ | 1.091 | 0.2871 | −0.3005 |
| $CHF_2OCH_2-H$ | 1.089 | 0.2884 | −0.3035 |
| $CF_3OCH_2-H$ | 1.089 | 0.2894 | −0.3056 |
| $CH_3OCHF-H$ | 1.094 | 0.2961 | −0.3163 |
| $CH_2FOCHF-H$ | 1.092 | 0.2976 | −0.3199 |
| $CHF_2OCHF-H$ | 1.092 | 0.2982 | −0.3214 |
| $CF_3OCHF-H$ | 1.091 | 0.2993 | −0.3241 |
| $CH_3OCF_2-H$ | 1.093 | 0.3045 | −0.3361 |
| $CH_2FOCF_2-H$ | 1.092 | 0.3059 | −0.3398 |
| $CHF_2OCF_2-H$ | 1.092 | 0.3062 | −0.3404 |
| $CF_3OCF_2-H$ | 1.092 | 0.3072 | −0.3437 |

**TABLE 4: Calculated Properties at the O−H$^+$ Bond Critical Point. Distances in angstroms and the Remaining Properties in au**

| complex | $r_{OH}$ | $\rho_c$ | $100\epsilon$ | $H_c$ | $\lambda_1$ | $\lambda_2$ | $\lambda_3$ |
|---|---|---|---|---|---|---|---|
| **1**+ | 0.9759 | 0.3493 | 2.46 | −0.6012 | −1.9122 | −1.8664 | 1.6033 |
| **2**+ | 0.9770 | 0.3459 | 2.29 | −0.5939 | −1.8913 | −1.8490 | 1.5902 |
| **3**+ | 0.9814 | 0.3411 | 2.28 | −0.5907 | −1.8813 | −1.8394 | 1.5823 |
| **4**+ | 0.9828 | 0.3402 | 2.38 | −0.5890 | −1.8807 | −1.8370 | 1.5785 |
| **5**+ | 0.9799 | 0.3427 | 2.24 | −0.5863 | −1.8674 | −1.8264 | 1.5739 |
| **6**+ | 0.9814 | 0.3408 | 2.13 | −0.5839 | −1.8599 | −1.8212 | 1.5678 |
| **7**+ | 0.9828 | 0.3380 | 2.17 | −0.5818 | −1.8581 | −1.8185 | 1.5655 |
| **8**+ | 0.9838 | 0.3364 | 2.15 | −0.5759 | −1.8380 | −1.7993 | 1.5520 |
| **9**+ | 0.9828 | 0.3369 | 2.26 | −0.5804 | −1.8522 | −1.8112 | 1.5585 |
| **10**+ | 0.9839 | 0.3342 | 2.31 | −0.5787 | −1.8507 | −1.8089 | 1.5558 |

**TABLE 5: Bond Ellipticities at the C−O Bond Critical Points in the Neutral (M) and Protonated (MH$^+$) Species**

| | $10^3\epsilon$ (O−C1) | | $10^3\epsilon$ (O−C2) | |
|---|---|---|---|---|
| complex[a] | M | MH$^+$ | M | MH$^+$ |
| **1** | 25 | 15 | 25 | 16 |
| **2(g)(a)** | 14 | 15 | 182 | 277 |
| **2(g)(b)** | | 15 | | 286 |
| **2(t)** | 8 | | 238 | |
| **3** | 0 | 37 | 47 | 103 |
| **4** | 4 | 38 | 60 | 40 |
| **5** | 206 | 47 | 206 | 281 |
| **6(a)** | 222 | 308 | 63 | 129 |
| **6(b)** | | 254 | | 116 |
| **7(a)** | 243 | 306 | 46 | 36 |
| **7(b)** | | 288 | | 37 |
| **8** | 89 | 308 | 89 | 130 |
| **9** | 97 | 104 | 34 | 34 |
| **10** | 33 | 129 | 33 | 34 |

[a] (t) and (g) respectively denote trans and gauche conformers of molecule **2**. (a) and (b) denote two possible protonations (see Table 1).

increase in the order: **1** and **2t** (no F/F or F/H 1,5-dispositions), **2** (one F/H), **3**-**5** (two F/H), **6**-**7** (one F/F and F/H), **8**-**10** (two F/F 1,5-dispositions). On the contrary, the evolution of the C−O−C bond angle cannot be related to the magnitude of the positive charges, $q$(C), of the carbons (Table 7).

As we have previously reported for a series of protonated unbranched alkyl monoethers,[28] protonation induces an appreciable stretching on C−O bonds. However this is not the most meaningful geometrical effect introduced by protonation. As it has been previously reported,[7] we have also found that some of the polyfluorinated compounds experience a substantial relative reorientation of the $CH_nF_{3-n}$ groups upon protonation. The extent of this reorientation is measured by the $w_{F-C1}\cdots$C2−F parameter (Table 2). It can be observed that the largest values take place in those molecules where the protonation results in a larger decrease of the antiperiplanar dispositions of

**TABLE 6: Calculated Protonation Energies at B3LYP/6-31++G(d,p) Level ($\Delta E$), Proton Charges and Energies in the Molecules Studied: Energies in kJ mol$^{-1}$ and Charges in au**

| complex | $\Delta E$ | $q$(H$^+$) | $E$(H$^+$) |
|---|---|---|---|
| **1** | −821.42 | 0.673 | −813.64 |
| **2** | −768.67 | 0.677 | −800.51 |
| **3** | −725.66 | 0.679 | −796.58 |
| **4** | −691.85 | 0.691 | −773.73 |
| **5** | −721.01 | 0.678 | −795.53 |
| **6** | −690.29 | 0.682 | −787.39 |
| **7** | −658.56 | 0.690 | −772.42 |
| **8** | −668.82 | 0.687 | −772.68 |
| **9** | −633.38 | 0.692 | −766.91 |
| **10** | −603.21 | 0.700 | −752.73 |

**TABLE 7: Electron Population (au) of Atomic Basins in the Neutral Species**

| molecule | $N$(C1) | $N$(O) | $N$(C2) |
|---|---|---|---|
| **1** | 5.427 | 9.082 | 5.427 |
| **2(g)** | 5.464 | 9.093 | 4.875 |
| **2(t)** | 5.447 | 9.080 | 4.855 |
| **3** | 5.497 | 9.099 | 4.287 |
| **4** | 5.499 | 9.084 | 3.634 |
| **5** | 4.911 | 9.091 | 4.911 |
| **6** | 4.915 | 9.092 | 4.296 |
| **7** | 4.915 | 9.074 | 3.642 |
| **8** | 4.290 | 9.096 | 4.290 |
| **9** | 4.288 | 9.075 | 3.631 |
| **10** | 3.624 | 9.053 | 3.624 |

fluorine atoms to an oxygen lp (**8**−**10**), which reduces the $n_O\rightarrow\sigma^*_{C-F}$ hyperconjugative delocalization. In the neutral molecule, the stabilization due to these hyperconjugative delocalizations is larger than fluorine/fluorine repulsions, which yields F−C$_1\cdots$C$_2$−F dihedral angles of zero degrees. After protonation, the number of these anomeric antiperiplanar interactions is reduced (from 4 to 2 in **8**−**10**) and they do not compensate for the F−F repulsions. This results in a reorientation in the relative position of the terminal groups. This reorientation was previously related to a possible O−H$^+\cdots$F hydrogen bond.[7] This consideration, however, has never been confirmed. In this work, we have looked for the corresponding F−H$^+$ bond critical points, nevertheless no one of these points were obtained, though really unexpected attractor interaction lines have been previously described in several systems.[36−38]

Though the full optimized most stable rotamers of the neutral symmetrically substituted molecules (**5**, **8**−**10**) have $C_{2v}$ geometry, the asymmetry introduced by the protonation in **5**+ and the reorientation of the $CF_nH_{3-n}$ experienced in **8**+ and **5**+ lower the symmetry to a $C_1$ structure. So, the different values of lp-O−C$_1$−F and *lp*-O−C$_2$−F dihedral angles in these protonated molecules originate differing O−C$_1$ and O−C$_2$ bond lengths (Table 2). The shortest O−C bond lengths are displayed by those carbons with the largest number of lp-O−C−F antiperiplanar arrangements.

Protonation also opens the C−O−C bond angle, with the exception of compound **8**. The different values can be explained as the result of a simultaneous increasing of the steric repulsions and decreasing of the hyperconjugative delocalizations. The specific behavior of compound **8** for the evolution of the C−O−C angle in the protonation process can be rationalized by considering a decrease from 4 to 1 antiperiplanar *lp*-O−C−F arrangements. Two of them are lost because of the formation of the O−H$^+$ bond and another one due to the $CF_nH_{3-n}$ subsequent reorientation.

**B. Bond Properties.** The ability of HFEs to reacte with hidroxyl radicals is related[4] to the strength of the C−H bonds.

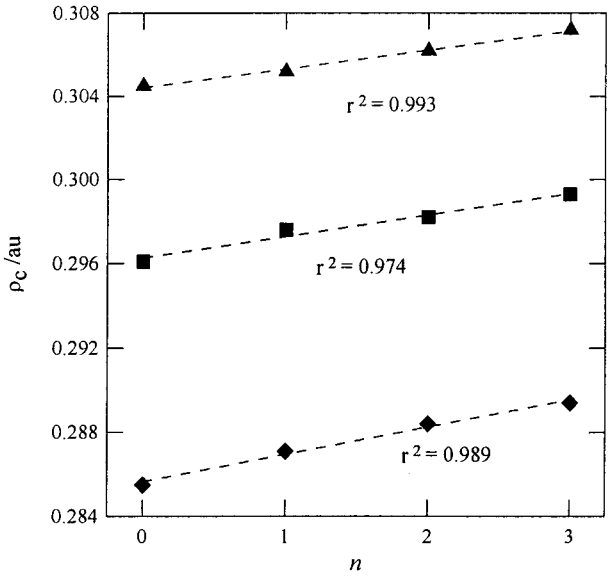


**Figure 2.** Plot of the charge density at the CH bond critical point versus the number $n$ of fluorine atoms in the molecule. (◆) $CH_{3-n}F_n$-$OCH_2$−H, (■) $CH_{3-n}F_nOCHF$−H, (▲) $CH_{3-n}F_nOCF_2$−H.

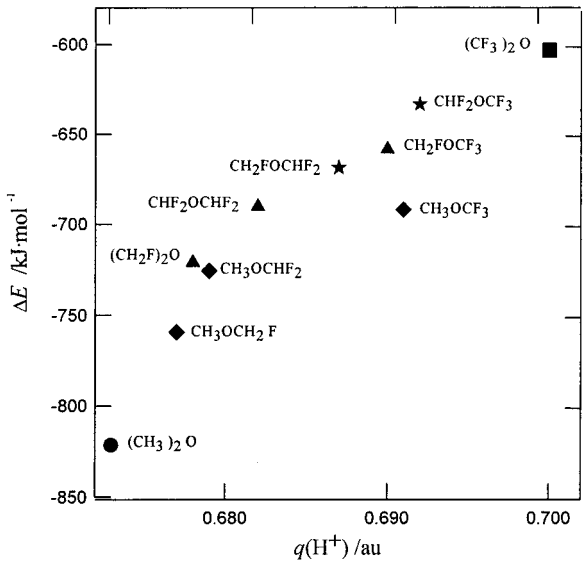


**Figure 3.** Variation of the calculated protonation energy ($\Delta E$) with the charge of the proton ($q(H^+)$).

Local properties of C−H bonds (hydrogen atom in trans position with regard to the C−O−C plane) have been summarized in Table 3. It can be observed there how stepwise-fluorination induces noticeable changes on C−H bond properties. As derived from the calculated values of bond distance, charge density and total energy density at the bond critical point, the strength of C−H bonds rises as the overall number of fluorine atoms in the molecule increases. This is in accordance with the results of the above-mentioned thermochemical study of C−H bond strengths.[4] Holding the number of fluorine atoms on a methyl group fixed at any value (0, 1, or 2) and increasing the fluorine content on the other methyl group, a reasonable linear correlation is found between the calculated values of the charge density $\rho_c$ and the number of fluorine atoms, as illustrated in Figure 2. The slopes of the linear regression equations for $CH_{3-n}F_n$-$OCH_2$−H, $CH_{3-n}F_nOCHF$−H and $CH_{3-n}F_nOCF_2$−H series are 0.0013 au, 0.0010 au and 0.0009 au, respectively, which are very similar, within the numerical precision of the calculations. Predictably, the effect of geminal fluorination on C−H bond properties is more marked than vicinal F-substitution. We have computed a rising of about 0.01 au in the calculated value of $\rho_c$ per adjacent fluorination step against an average increment of about 0.001 au per fluorination step on the other methyl group. The total energy density at the bond critical point, $H_c$, has proven to be a useful parameter to classify the character of atomic interactions.[39] $H_c$ values along this series also reflect how the strength of the C−$H_{anti}$ bond rises with increasing fluorination.

Local properties at the O−$H^+$ bond critical points for the cation series are given in Table 4. In contrast to C−H bonds, the calculated values of the O−$H^+$ bond distance, $r_{OH}$, are found to increase as the overall number of fluorine atoms increases (on going from $(CH_3)_2O$ to $(CF_3)_2O$, $r_{OH}$ undergoes an increase of 0.008 Å). This is expected, since, in contrast to alkyl groups, fluorine atoms are not electron donors and they withdraw electron charge from O−$H^+$ bond, destabilizing it.

As was previously found by Wiberg and Breneman,[40] the values of $\rho_c$ at the bond critical point are correlated with $r_{OH}$ since a shorter bond leads to increased overlap and therefore larger values of $\rho_c$. Examination of Table 4 reveals substantial variations in the calculated values of the two negative eigenvalues of the Hessian at the O−$H^+$ bond critical point, $\lambda_1$ and $\lambda_2$ along the series. The values of the ellipticity of the bond $\epsilon$ (related in the AIM theory to the $\pi$ character of the bond)[16] are found, however, to be remarkably constant. The curvature parallel to the bond path, $\lambda_3$, is found to decrease as the fluorine content increases, consistently with the values of the bond order previously discussed, which indicates that the $OH^+$ bond in dimethyl ether is more resistant to the changes in the molecule environment than in the fluorinated forms. The calculated $H_c$ values, as corresponding to a covalent interaction, are negative and their absolute value decrease with increasing $r_{OH}$ (i.e., the bond order decreases).

The ellipticities of the O−C bonds (Table 5) display substantial changes along the series. Though these changes should be expected according to an interpretation of the O−C−F anomeric effect made exclusively in terms of $n_O \rightarrow \sigma^*_{C-F}$ hyperconjugative delocalization, they do not follow the relative changes predicted by this interaction. In fact, according to that effect O−$C_2$ ellipticity should be larger in gauche rotamer of **2** than in the anti one, and the reverse is found. Also protonation at the opposite side of the C−O−C plane (with regard to the F atom) should reduce O−$C_2$ ellipticity, whereas it is really enlarged in magnitude that is almost the same for any protonation site. All these facts lead us to conclude, as Werstiuk et al. did for O−C−O,[17] though based only on the analysis of the charge density topology, that the F−C−O anomeric interaction cannot be derived only from a $n_O \rightarrow \sigma^*_{C-F}$ hyperconjugative delocalization.

**C. Protonation Energies.** The calculated protonation energies, uncorrected for the zero-point vibrational energy (ZPVE), at the B3LYP/6-31++G(d,p) level are presented in Table 6, which also displays the charges, $q(H^+)$, and energies, $E(H^+)$, on the proton. These values are obtained by integrating the corresponding density property function over the $H^+$ basin (Figure 5). Experimental gas-phase PA is only available for $(CH_3)_2O$ molecule,[41] (792.0 kJ $mol^{-1}$). The uncorrected protonation energy for this complex (−821.4 kJ $mol^{-1}$), decreases after ZPVE correction to −786.9 kJ $mol^{-1}$, which gives a closer agreement to the experimental value. To compare with previous calculations, it is worth adding that Orgel et al.[7] have reported a proton affinity of 810.7 kJ $mol^{-1}$ computed at the MP2/6-31G(d,p) level, further from the experimental value. As a general

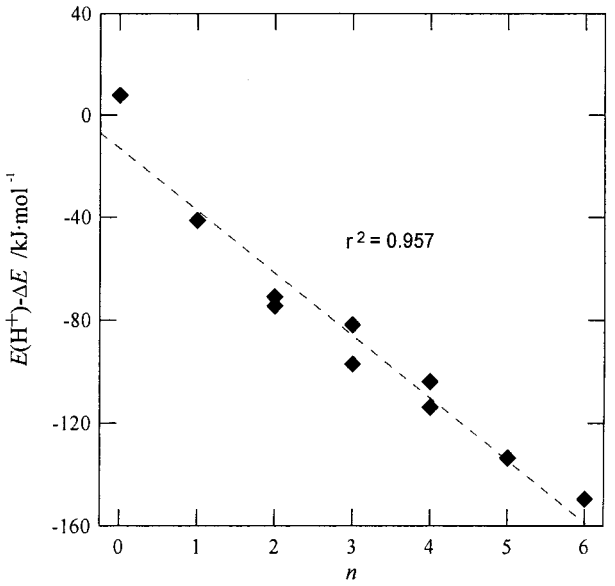


**Figure 4.** Plot of the energy of the proton minus the calculated protonation energy ($E(H^+)-\Delta E$) against the number of fluorine atoms in the molecule.

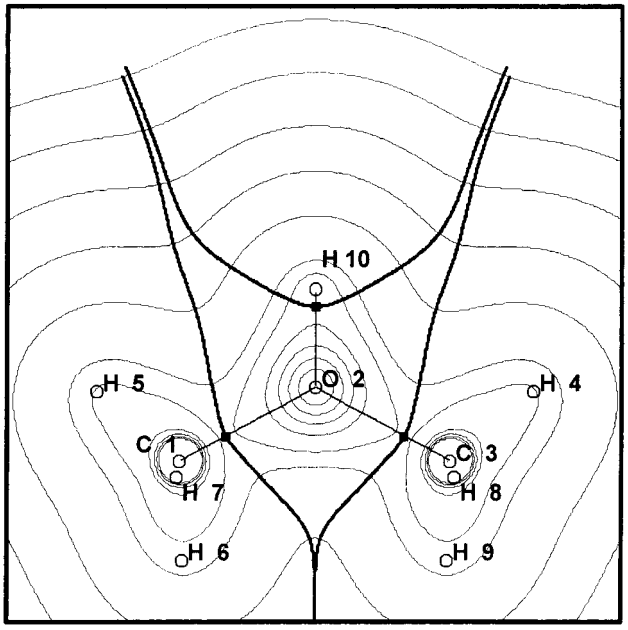


**Figure 5.** Superposition of the contour lines (thin) of the charge density (1.0, 0.8, 0.6, 0.4, 0.2, 0.1, $10^{-2}$, $10^{-3}$, $10^{-4}$, $10^{-5}$, and $10^{-6}$ au from the most internal to the most external contours) with the projection of the molecular graphs (bold) and interatomic surfaces (bold) over the plane defined by the O2−C1, O2−C3, and O2−H10$^+$ bond critical points for the $OH^+$ region of dimethyl ether, **1**. Projection of the nuclei are represented by (●) and (■) represents the locations of bond critical points. $N(H^+)$ and $E(H^+)$ are integrated over the space bounded by the $10^{-6}$ au contour line of the charge density and the interatomic surfaces containing H10 nucleus. Plot made with MORPHY98.[46]

trend, computed PAs decrease as the fluorine content in the molecule is increased. Though it has to be born in mind that any neutral species with a lone pair is a potential Lewis base, it can be said, as it has been previously predicted,[7] that under usual circumstances a heavily fluorinated ether would act as a relative poor Lewis base. In fact, if we assume that the difference between experimental PA and ZPVE uncorrected computed PA in **1** is a good estimation of this difference along this series, the PA of the perfluorinated ether **10** would decrease to somewhat 573 kJ.mol$^{-1}$, which is between ethane (596.3 kJ.mol$^{-1}$) and methane (543.5 kJ.mol$^{-1}$) PA.[42]

According to the AIM study, after protonation, a substantial positive charge (always larger than $^2/_3$ au) remains on the hydrogen atom attached to the oxygen, as it is illustrated by Table 5 and also found in the oxygen protonation of other series of compounds.[28,43] This result exactly means that the atomic basin of that hydrogen (Figure 5) carries a very small electron population. A similar result is found for the $[H_3O]^+$ cation at the same level ($N(H) = 0.272$ au, $N(O) = 9.184$ au). So, the AIM results do not support the widespread description of protonated ethers as dialkyloxonium cations with an $O^+-H$ bond ($RR'O^+H$), and suggest that the charge distribution in the $(RR'OH)^+$ species is closer to a $RR'OH^+$ structure than to a $RR'O^+H$. Both $RR'OH^+$ and $RR'O^+H$ structures correspond to the initial and final states of the formal process $ROR' + H^+ \rightarrow (ROR')^+ + H$. Its reaction energy is the difference between the ROR′ and H ionization potentials (IP). Though ROR′ present lower IPs than H (they are estimated to range from 6.8 in **1** to 10.6 eV in **10** by using Koopman's theorem), the position of the energy minimum (represented by the amount of charge transferred to $H^+$ basin) in this formal process is placed (according to the AIM results) closer to the $RR'OH^+$ form. Once more, the AIM theory yields results that are not in keeping with the view of the traditional resonance theory. In this line, Wiberg and Laidig concluded that no charge transfer from the nitrogen to the carbonyl oxygen is involved in the nature of the interaction between an amino group and a carbonyl in an amide.[44]

As it has been reported for a series of protonated linear alkyl monoethers,[28] we find a linear correlation between the calculated protonation energy $\Delta E$ and the charge on the proton $q(H^+)$. This is in agreement with the fact that the most important contribution to proton affinities comes from charge transfer, rather than dipole interaction.[45] The charges at all other atoms are affected by the molecule environment and hence their charge is roughly correlated with the protonation energies. Protonation energies can also be related to the proton energies, which are given in Table 5. In the case of dimethyl ether, the energy of this atom accounts for 94% of the protonation energy. For the fluorinated species, the energy of the proton exceeds, in absolute value, that of the computed protonation energy and the magnitude of this difference increases with the fluorine content in the molecule. This means the rest of the system is destabilized because electron charge is withdrawn from it (a subsystem containing several electronegative atoms).

**D. Electron Atomic Populations.** Due to the electron charge withdrawal from carbon atoms, the oxygen has a negative charge of 1.082 au in dimethyl ether. Table 7 shows that the substitution of only one or two of the hydrogen atoms (gauche to the C−O−C chain) with fluorine yields to a very small increase of the oxygen negative charge, whereas the substitution of the hydrogen closest to the C−O−C plane results in an, also very small, decrease of $N(O)$. This fact is also against $n_O \rightarrow \sigma^*_{C-F}$ hyperconjugative delocalization is the dominant effect in aliphatic F−C−O units.

The trends displayed by carbon charges, that show a big variation (clearly due to the high electronegative nature of F atoms bonded to them), parallel those concerning C−O bond distances. Thus, increasing the fluorine content on $C_2$ yields to increased values of $N(C_1)$, whereas the electron population on $C_2$ decreases. There is also an effect due to the lp-O−C−F arrangement. Table 7 shows that whenever a F atom is placed in a lp-O−C−F gauche arrangement it gives rise to an O charge depletion with regard to the most similar compound without

**TABLE 8: Variation of the Electron Population (au) of Atomic Basins upon Protonation[a]**

| atom | 1 | 2 | 3 | 4 | 5 | 8a | 10 |
|---|---|---|---|---|---|---|---|
| C1 | 0.201 | 0.188 | 0.171 | 0.170 | 0.115 | 0.059 | −0.025 |
| O | −0.054 | −0.084 | −0.114 | −0.105 | −0.106 | −0.142 | −0.121 |
| C2 | 0.199 | 0.131 | 0.055 | −0.020 | 0.112 | 0.056 | −0.026 |
| 1t | −0.099 | −0.095 | −0.100 | −0.089 | −0.091 | −0.111 | −0.026(F) |
| 1ga | −0.126 | −0.096 | −0.105 | −0.100 | −0.109 | −0.019(F) | −0.021(F) |
| 1gb | −0.110 | −0.117 | −0.085 | −0.086 | −0.024(F) | −0.022(F) | −0.021(F) |
| 2t | −0.099 | −0.097 | −0.092 | −0.029(F) | −0.091 | −0.099 | −0.024(F) |
| 2gb | −0.110 | −0.123 | −0.024(F) | −0.024(F) | −0.096 | −0.020(F) | −0.021(F) |
| 2ga | −0.126 | −0.027(F) | −0.027(F) | −0.026(F) | −0.030(F) | −0.016(F) | −0.024(F) |

[a] Every H or F atom is denoted by indicating the carbon to whom it is bonded (1 or 2), its disposition to the C−O−C chain (gauche, g, or trans, t), and their position with regard to the C−O−C plane and the $H^+$ (same side, a, opposite side, b). When a fluorine atom occupies the site, an F atom in brackets indicates it.

**TABLE 9: Energy, $E(\Omega)$, of the Main Atomic Basins in the Neutral Species (M) (au) and Variation of Its Energy upon Protonation, $\Delta E(\Omega)$ (kJ mol$^{-1}$)**

| molecule | $E$(C1) | $E$(O) | $E$(C2) | $\Delta E$(C1) | $\Delta E$(O) | $\Delta E$(C2) |
|---|---|---|---|---|---|---|
| **1** | −37.6939 | −75.8616 | −37.6935 | −340.0 | 4.5 | −341.3 |
| **2** | −37.6857 | −75.8466 | −37.3169 | −308.2 | 149.9 | −201.4 |
| **3** | −37.6869 | −75.8626 | −36.8885 | −284.9 | 279.1 | −17.9 |
| **4** | −37.6809 | −75.8735 | −36.3795 | −284.6 | 305.9 | 126.3 |
| **5** | −37.3294 | −75.8511 | −37.3296 | −159.6 | 251.0 | −143.6 |
| **6** | −37.3137 | −75.8772 | −36.8855 | −168.3 | 375.4 | −7.4 |
| **7** | −37.3079 | −75.8865 | −36.3726 | −175.1 | 397.8 | 137.6 |
| **8** | −36.8659 | −75.8909 | −36.8654 | −44.6 | 409.3 | −34.7 |
| **9** | −36.8609 | −75.9033 | −36.3543 | −20.5 | 473.9 | 122.1 |
| **10** | −36.3425 | −75.9126 | −36.3425 | 116.6 | 487.0 | 117.4 |

this substitution (i.e., compare $N$(O) for **2t** and **1** or those of **4** and **3** in Table 7). The reverse holds whenever the F atom is placed in a lp-O−C−F trans arrangement.

Protonation leads to a sizable distortion of the neutral molecule charge density, which is reflected in noticeable changes in the computed electron populations. After protonation, the negative charge of oxygen atom decreases. The charge of carbon atoms becomes less positive, except for the fully fluorinated carbons. As was previously deduced for aldehydes, ketones,[43] and ethers,[28] the hydrogens are the atoms most affected by the charge withdrawal accompanying protonation. Also, the protonation of $H_2O$ results in reducing $N$(H) from 0.421 to 0.272 au (in this case $N$(O) is even increased by the protonation in $2.6\cdot\times 10^{-3}$ au). Table 8 shows the changes exhibited by $N(\Omega)$ ($\Delta N(\Omega)$) for all the atoms in several selected molecules. For dimethyl ether **1**, protonation takes place by increasing the electron population of C atoms and decreasing the remaining. The largest loss of charge corresponds to the hydrogens, especially those in gauche and **a** arrangements (Table 8). When a C is partially fluorinated it also increases $N$(C) upon protonation while the F atoms lost electron charge. Nevertheless, in those compounds with perfluorinated C, the electron population on that C is reduced by the protonation (C2 in **4** or C1 and C2 in **10**). In the perfluorinated molecule **10**, the charge lost for every carbon atom is about the same as the one lost for every F, while 40% of the charge withdrawal comes from the oxygen atom. It is worth to mention that $\Delta N$(F) presents much smaller variations along the series than $\Delta N$(C) or $\Delta N$(O) (in fact, the charge lost by the oxygen atom is normally increased with the number of fluorines).

**E. Atomic Energies.** The atomic energies of the O−C−O unit (Table 9) allow us to describe the following trends.

*(a)* A larger number of fluorine atoms in the molecule stabilizes the oxygen in the neutral molecules and destabilizes it in the protonated species.

*(b)* As a general rule, the carbon atoms (both in the neutral and protonated forms) are slightly destabilized by an increasing number of fluorine atoms linked to the other carbon and to a much greater extent by increasing its own fluorine substitution (Figure 6).

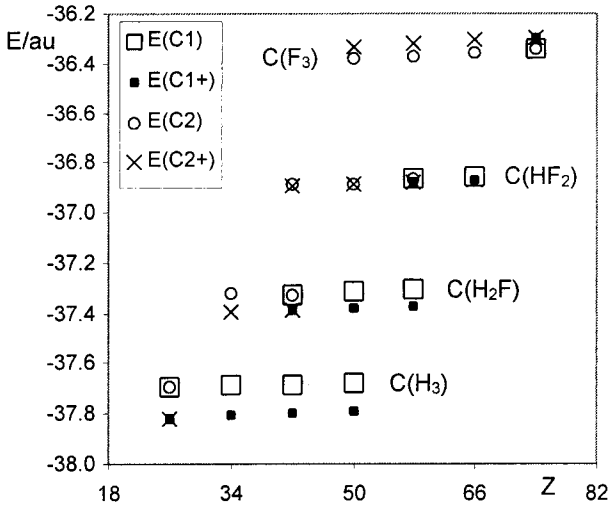


**Figure 6.** Energy of the carbon atoms in protonated and unprotonated species vs. sum of the atomic numbers in the molecule ($Z$).

*(c)* Regarding the protonation process, the oxygen atom is always destabilized. A larger number of fluorine substituents results in a larger oxygen destabilization. On the other hand, carbon atoms are stabilized after the protonation process when they are partially fluorinated. The stabilization clearly decreases as fluorine replaces a larger number of hydrogens and results in destabilizing perfluorinated carbons (Table 9). The percentage due to O or C destabilization in the total protonation energy present large variations along this series, in contrast to what happened to the energy of the proton.

## 5. Conclusions

A detailed examination of the effects brought about by fluorine substitution on the properties related to the electron charge density of fluorinated dimethyl ethers yielded the following major conclusions.

**1.** The topological analysis of the charge density reveals that there is no interaction line between the proton and any of the fluorine atoms in the protonated forms of fluorinated dimethyl ethers. Reorientation of the $CF_nH_{3-n}$ groups upon protonation is explained as result of the balance between steric and anomeric interactions.

**2.** The values of the atomic and bond properties computed with the AIM theory have been applied to rationalize some anomeric geometrical and conformational trends. These values are in agreement with a complex origin of the O−C−F anomeric

effect, which cannot be exclusively interpreted in terms of $n_O \rightarrow \sigma^*_{C-F}$ hyperconjugative delocalization.

**3.** Fluorine substitution leads to an increase of C−H bond strengths and therefore heavily fluorinated methyl ethers, when used as refrigerants and because of their lower affinity for hydroxyl radicals, may contribute to the global warming.

**4.** The calculated protonation energies were found to correlate well with the charges on the proton, which supports the fact that protonation is mainly determined by charge transfer.

**5.** Increasing the fluorine content results in substantial changes in the computed values of the electron populations of the oxygen and carbon atoms, though the fluorine atoms undergo significantly smaller variations of their electron population.

**6.** After the protonation process, the proton is attached to the molecule keeping a very high positive charge. Its electron population is withdrawn mainly from hydrogen and oxygen atoms, while carbon atoms even increase their atomic population in this process if we exclude heavily fluorinated compounds.

**7.** Fluorine substituents destabilize the carbon atoms (especially the one linked to them) in neutral and protonated species, whereas the oxygen is stabilized in the neutral form and destabilized in the protonated one.

**Acknowledgment.** This work was partially supported by *Xunta de Galicia*. We thank to the *Centro de Supercomputación* de Galicia for the allocation of computational resources. María De la Puente and Miguel De la Puente are also thanked for helpful discussions regarding this work.

## References and Notes

(1) The Ozone Secretariat. The Montreal Protocol on Substances that deplete the Ozone. (http://www.unep.ch/montreal.htm).

(2) Zhang, Z.; Saini, R. D.; Kurylo, M. J.; Huie, R. E. *J. Phys. Chem.* **1992**, *96*, 9301.

(3) Bartolotti, L. J.; Edney, E. O. *Int. J. Chem. Kinet.* **1994**, *96*, 913.

(4) Lazarou, Y. G.; Papagiannakopoulos, P. *Chem. Phys. Lett.* **1999**, *301*, 19.

(5) Good, D. A.; Francisco, J. S.; Jain, A. K.; Wuebbles, D. J. J. *Geophys. Res.* **1998**, *103*, 28181.

(6) Good, D. A.; Francisco, J. S. *J. Phys. Chem. A* **1998**, *102*(10), 1854.

(7) Orgel, V. B.; Ball, D. W.; Zehe, M. J. *J. Mol. Struct. (THEOCHEM)* **1997**, *417*, 195.

(8) Fontaine, M.; Delhalle, J.; Defranceschi, M.; Bourin, J. M. *J. Mol. Struct.* **1993**, *300*, 607.

(9) Pacansky, J.; Miller, M.; Hatton, W.; Liu, B.; Scheiner, A. *J. Am. Chem. Soc.* **1991**, *113*, 329.

(10) Kirby, A. J. *The Anomeric Effect and Related Stereoelectronic Effects at Oxygen*; Springer-Verlag: Berlin, 1983.

(11) Edward, J. T. *Chem. Ind.* **1955**, *33*, 1102.

(12) Salzner, U.; Schleyer, P. v R. *J. Am. Chem. Soc.* **1993**, *115*, 10231.

(13) Gorenstein, D. G. *Chem. Rev.* **1987**, *87*, 104.

(14) Suarez, D.; Sordo, T. L.; Sordo, J. A. *J. Am. Chem. Soc.* **1996**, *118*, 9850.

(15) Carballeira, L.; Pérez-Juste, I. *J. Org. Chem.* **1997**, *62*, 6144.

(16) Bader, R. F. W. *Atoms in Molecules. A Quantum Theory*; Clarendon: Oxford, 1990.

(17) Werstiuk, N. H.; Laidig, K. E.; Ma, J. *The Anomeric Effect and Associated Stereoelectronic Effects*; ACS Symposium Series 539; American Chemical Society: Washington, DC, 1993; Chapter 10, p 176.

(18) Bader, R. F. W. *Chem. Rev.* **1991**, *91*, 893.

(19) Bader, R. F. W. *Pure Appl. Chem.* **1988**, *60*, 145.

(20) Sbrenik, S.; Bader, R. F. W.; Nguyen-Dang, T. T. *J. Chem. Phys.* **1978**, *68*, 3667.

(21) Frisch, M. J.; Trucks, G. W.; Schlegel, H. B.; Gill, P. M. W.; Johnson, B. G.; Robb, M. A.; Cheeseman, J. R.; Keith, T.; Petersson, G. A.; Montgomery, J. A.; Raghavachari, K.; Al-Laham, M. A.; Zakrzewski, V. G.; Ortiz, J. V.; Foresman, J. B.; Cioslowski, J.; Stefanov, B. B.; Nanayakkara, A.; Challacombe, M.; Peng, C. Y.; Ayala, P. Y.; Chen, W.; Wong, M. W.; Andres, J. L.; Replogle, E. S.; Gomperts, R.; Martin, R. L.; Fox, D. J.; Binkley, J. S.; Defrees, D. J.; Baker, J.; Stewart, J. P.; Head-Gordon, M.; Gonzalez, C.; Pople, J. A. *Gaussian 94*, Revision C.3; Gaussian, Inc.: Pittsburgh, PA, 1995.

(22) Kohn, W.; Sham, L. J. *Phys. Rev.* A **1965**, *140*, 1133.

(23) Becke, A. D. *J. Chem. Phys.* **1993**, *98*, 5648.

(24) Lee, C.; Yang, W.; Parr, R. G. *Phys. Rev. B* **1988**, *37*, 785.

(25) Durig,. R.; Liu, J.; Guirgis, G. A.; van der Veken, B. J. *Struct. Chem.* **1993**, *4*(2)103.

(26) Lias, S. G.; Liebman, J. F.; Levin, R. D. *J. Phys. Chem. Ref. Data* **1984**, *13*, 695.

(27) Lias, S. G.; Bartmess, J. E.; Liebman, J. F.; Holmes, J. L.; Levin, R. D.; Mallard, W. G. *J. Phys. Chem. Ref. Data* **1988**, 14 Suppl. 1.

(28) Vila, A.; Carballo, E.; Mosquera, R. A. *Chem. Phys. Lett.* **2000**. In press.

(29) AIMPAC: A suite of programs for the Theory of Atoms in Molecules; Bader, R. F. W., and co-workers, Eds.; McMaster University: Hamilton, Ontario, Canada, L8S 4M1. Contact bader@mcmail.cis.mcmaster ca.

(30) Graña, A. M.; Mosquera, R. A. *J Chem. Phys.* **1999**, *110*, 6606.

(31) Vila, A.; Carballo, E.; Mosquera, R. A. *Can. J. Chem.* **2000**. In press.

(32) Harmony, M. D.; Laurie, V. W.; Kuckzkowski, R. L.; Schewendeman, R. H.; Ramsay, D. A.; Lovas, F. J.; Lafferty, W. J.; Maki, A. G. *J. Phys. Chem. Ref. Data* **1979**, *8*, 619.

(33) Kuchitsu, K.; Oyanagi, K. *Faraday Discuss. Chem. Soc.* **1977**, *62*, 20.

(34) Cioslowski, J.; Varnali, T. *Int. J. Quantum Chem.* **1999**, *72*, 331.

(35) Cioslowski, J.; Varnali, T. *J. Phys. Chem.* **1996**, *100*, 18725.

(36) Cioslowski, J.; Eddington, L.; Stefanov, B. *J. Am. Chem. Soc.* **1995**, *117*, 10381.

(37) Popelier, P. L. A.; Logothetis, G. *J. Organomet. Chem.* **1998**, *555*, 101.

(38) Bader, R. F. W. *J. Phys. Chem. A* **1998**, *102*, 7314.

(39) Cremer, D.; Kraka, E. *Croat. Chem. Acta* **1984**, *57*, 1259.

(40) Wiberg, K. B.; Breneman, C. M. *J. Am. Chem. Soc.* **1990**, *112*, 8765.

(41) Hunter, E. P.; Lias, S. G., In Protton Affinity Evaluations. *NIST Chemistry Webbook*; NIST Standard Reference Database 69; Mallard, W. G.; Linstrom, P. J. Eds.; National Institute of Standards and Technology: Gaithersburg, MD 20899, 1998 (http://webbook.nist.gov).

(42) Hunter, E. P.; Lias, S. G, *J. Phys. Chem. Ref. Data* **1998**, *27*, 413.

(43) Graña, A. M.; Mosquera, R. A. *Chem. Phys.* **1999**, *243*, 17.

(44) Wiberg, K. B.; Laidig, K. E. *J. Am. Chem. Soc.* **1987**, *109*, 5935.

(45) Hehre, W. J.; Taagepera, M.; Taft, R. W.; Topsom, R. D. *J. Am. Chem. Soc*. **1981**, *103*, 1344.

(46) MORPHY98, a topological analysis program written by P. L. A. Popelier with a contribution from R. G. A. Bone. UMIST: England.